



HAL
open science

Surface properties associated with the production of polysaccharides in the food bacteria *Propionibacterium freudenreichii*

Fanny Guyomarc'H, Gregory Francius, Sandrine Parayre, Marie-Noelle Madec, Stéphanie-Marie Deutsch

► To cite this version:

Fanny Guyomarc'H, Gregory Francius, Sandrine Parayre, Marie-Noelle Madec, Stéphanie-Marie Deutsch. Surface properties associated with the production of polysaccharides in the food bacteria *Propionibacterium freudenreichii*. *Food Microbiology*, 2020, 92, pp.103579. 10.1016/j.fm.2020.103579 . hal-02911595

HAL Id: hal-02911595

<https://hal.inrae.fr/hal-02911595v1>

Submitted on 4 Aug 2020

HAL is a multi-disciplinary open access archive for the deposit and dissemination of scientific research documents, whether they are published or not. The documents may come from teaching and research institutions in France or abroad, or from public or private research centers.

L'archive ouverte pluridisciplinaire **HAL**, est destinée au dépôt et à la diffusion de documents scientifiques de niveau recherche, publiés ou non, émanant des établissements d'enseignement et de recherche français ou étrangers, des laboratoires publics ou privés.



Distributed under a Creative Commons Attribution - NonCommercial - NoDerivatives 4.0 International License



Surface properties associated with the production of polysaccharides in the food bacteria *Propionibacterium freudenreichii*

Fanny Guyomarc'h^a, Grégory Francius^b, Sandrine Parayre^a, Marie-Noëlle Madec^a,
Stéphanie-Marie Deutsch^{a,*}

^a STLO, INRAE, Institut Agro, 35042, Rennes, France

^b Université de Lorraine, LCPME, Laboratoire de Chimie Physique et Microbiologie pour l'Environnement, UMR 7564, 54600, Villers-lès-Nancy, France

ARTICLE INFO

Keywords:

Polysaccharide
Exopolysaccharide
Surface properties
AFM
Propionibacterium freudenreichii
Cell wall

ABSTRACT

This study explores the production of polysaccharides (PS) in the strain Pf2289 of the food species *Propionibacterium freudenreichii*. Pf2289 presents characteristics atypical of the species: a molar-shaped morphotype upon plating, and cells strongly aggregative in liquid medium. When plating Pf2289, another morphotype was observed with a 4% frequency of appearance: round-shaped colonies, typical of the species. A clone was isolated, designated Pf456. No reversibility of Pf456 towards the molar-shaped morphotype was observed. Pf2289 was shown to produce a surface polysaccharide (PS) bound to the cell wall, mainly during the stationary growth phase. Meanwhile, Pf456 had lost the ability to produce the PS. AFM images of Pf2289 showed that entangled filaments spread over the whole surface of the bacteria, whereas Pf456 exhibited a smooth surface. Adhesion force maps, performed with concanavalin-A grafted probes, revealed twice as much adhesion of Pf2289 to concanavalin-A compared to Pf456. Furthermore, the length of PS molecules surrounding Pf2289 measured at least 7 μm, whereas it only reached 1 μm in Pf456. Finally, the presence of PS had a strong impact on adhesion properties: Pf2289 did not adhere to hydrophobic surfaces, whereas Pf456 showed strong adhesion.

1. Introduction

The cell wall is a key component of bacteria. It constitutes the interface between the extracellular environment and the bacteria, and plays a fundamental role in their physiology by making it possible to resist internal pressure by maintaining the shape of the cell, and as a barrier against external aggressions. In Gram-positive bacteria, which include most food bacteria, it is composed of a thick layer of peptidoglycan that can be decorated with diverse compounds: proteins, teichoic acids, lipoteichoic acids, polysaccharides and pili (for a review of LAB cell walls, see Chapot-Chartier and Kulakauskas (2014), and of Gram-positive bacteria, see Rajagopal and Walker (2017)). Of all of the compounds that decorate the cell wall's peptidoglycan, polysaccharides (PS) are among the most remarkable. They constitute a very rich diversity of macromolecules in terms of sugar composition, linkage or ramification, and length. Furthermore, the production of PS is species- but also strain-dependent, thus determining the peculiar surface properties of producing strains. Some strains have also demonstrated the ability to produce different types of PS. This was seen for the

Lactobacillus johnsonii strain FI9785, which produces two different PS: one branched dextran and one heteropolymer composed of galactose and glucose (Dertli et al., 2013). This is also the case for the well-studied probiotic strain *Lactobacillus rhamnosus* GG, which produces a major PS, a galactose-rich and high molecular weight molecule, as well as a minor low molecular weight and glucose-rich PS (Francius et al., 2008; Landersjö et al., 2002; Lebeer et al., 2009). In addition to the biological role they play in the producing cell, PS are also studied for the role they play in reinforcing specific properties. In the case of food bacteria, research has focused on PS-producing bacteria as a way to improve the texture of fermented foods such as cheese, yogurt (Mende et al., 2016) and bread (Galle and Arendt, 2014). Studies have also found that PS can have health-promoting properties related to their specific interaction with lectin-like receptors on dendritic cells (Lebeer et al., 2008).

Propionibacterium freudenreichii (Pf) is a food-grade bacterium with generally recognized-as-safe status (GRAS) that belongs to the class of dairy propionibacteria (Scholz and Kilian, 2016; von Freudenreich and Orla-Jensen, 1906). It is traditionally and most commonly used as a starter for the manufacture of hard cheeses such as Emmental and

* Corresponding author.

E-mail address: stephanie-marie.deutsch@inrae.fr (S.-M. Deutsch).

Leerdammer (Thierry et al., 2011) in which it contributes to the development of aromatic properties (Pogacic et al., 2015; Thierry et al., 2004). *Pf* is furthermore known to be a strong producer of vitamin B12 (Fang et al., 2017; Martens et al., 2002), and the first sequencing of a *Pf* genome led to the identification of the genes implicated in the biosynthesis of this vitamin (Falentin et al., 2010). It is also studied as a bio-protective agent due to the production of lactic, acetic and propionic acids during growth (Le Lay et al., 2016; Lind et al., 2005). Finally, *Pf* has attracted attention as a potential probiotic (Rabah et al., 2017). For this latter use of *Pf*, the cell wall composition is determinant. For example, in the context of chronic inflammatory bowel disease, *Pf*'s anti-inflammatory properties have been shown to be strongly strain-dependent (Foligné et al., 2010; Deutsch et al., 2017). In three strains of *Pf* that were shown to produce a cell wall PS composed of β -glucan, it was found that this PS masked the actors of the anti-inflammatory properties and that the removal of the PS by gene inactivation made it possible to reveal these actors (Deutsch et al., 2010, 2012). In the strain *Pf* UF1, Ge et al. (2020) showed that the glycosylation at the surface of the protein LspA regulates colonic dendritic cells, which are implicated in the T cell response to pathogen infections. PS molecules are therefore key actors of the surface properties of *Pf*.

A description of the strain-dependent variety of surface properties exhibited by *Pf* bacteria is therefore important to provide keys for users who want to choose strains for specific uses, e.g., in food or probiotic applications. In this study, we attempted to gain insight into the surface properties of *Pf* associated with the production of a PS. For this purpose, we studied an atypical strain of *Pf*, CIRM BIA 2289, which produces a cell wall PS that gives it an original morphotype. A spontaneous variant unable to extensively produce the PS was identified and we investigated the surface properties of both bacteria with AFM imaging, force spectroscopy and other classical methods.

2. Materials & methods

2.1. Strains and growth conditions

The *P. freudenreichii* CIRM BIA 2289 strain and its derivative CIRM BIA 456 (respectively abbreviated as *Pf* 2289 and *Pf* 456) are stored in the collection of the Centre International de Ressources Microbiennes-Bactéries d'Intérêt Alimentaire (CIRM-BIA; STLO, INRAE, Rennes, France). They were routinely grown at 30 °C in YEL broth (Malik et al., 1968) in closed glass tubes without agitation. Such conditions are generally described as "microaerophilic" and are optimal for dairy propionibacteria. Before use, the strains were subcultured from frozen stock, once on YEL medium and then once on the desired medium, using a 2% inoculum. In addition to YEL, YEL derivative mediums were used: a YEL medium supplemented with lactose at a final concentration of 45 g l⁻¹ (named YEL-lactose), and a YEL without lactate but with 45 g l⁻¹ of lactose (referred to as YE-lactose). For use in Petri dishes, YEL, YEL-lactose and YE-lactose were supplemented with agar (10 g l⁻¹). Finally, we used a dairy-based medium, referred to as UF-lac, constituted of a cow skim milk ultrafiltrate supplemented with 50 mM of sodium L-lactate (galaflo SL60; Société Arnaud, Paris, France) and 10 g l⁻¹ of casein hydrolysate (Organotechnie, La Courneuve, France), and sterilized by filtration (0.22 μ m). For use in Petri dishes, agar was added at a final concentration of 10 g l⁻¹, and the medium was autoclaved for sterilization.

2.2. Enumeration

Counting of colony-forming units (CFUs) via plate was performed as previously described by Yee et al. (2014). Briefly, serial ten-fold dilutions of 1 ml of the sample were performed in 0.1% sterile tryptone water. For each dilution, two Petri dishes of agar medium were incubated anaerobically at 30 °C for 6 days.

2.3. Immunoagglutination test

Agglutination tests were performed using an anti-*S. pneumoniae* serotype 37 antiserum raised against the β -glucan capsule of the bacteria (obtained from the Statens Serum Institute, Hillerød, Denmark). *P. freudenreichii* strains were grown in growth medium YEL or UF-lac, and the assays were performed as previously described (Walling et al., 2005).

2.4. Morphotypes of *P. freudenreichii*

The strain *Pf* 2289 or *Pf* 456 was grown at 30 °C on liquid medium (UF-lac or YEL) until the stationary growth phase (about 48 h of growth). The culture was then plated on YEL agar or UF-lac agar Petri dishes so as to have 20 to 200 colonies per plate. The Petri dishes were incubated for 5 days at 30 °C under anaerobic conditions. The clones were observed individually with respect to their shape, circularity and color. They were then counted with respect to the occurrence of distinct morphotypes.

2.5. Dry mass of bacterial cells of *Pf* during growth

Cultures of *Pf* were grown on liquid medium, UF-lac or YEL, at 30 °C, in calibrated tubes. During growth, tubes of culture were taken and centrifuged (7000 \times g, 15 min, 4 °C). After removal of the supernatant, the samples were dried in a fan-assisted speed-vac at 60 °C for 24 h, or until the mass of samples was stable. The dry mass of bacterial cells was calculated as the mass difference between the dry pelleted cells and the mass of the empty tube. In parallel, the bacterial concentrations were determined by CFU counting on YEL agar, as described in Section 2.2. As of 24 h, the cultures were sonicated, as described in Section 2.6, prior to enumeration. The dry mass experimentation was performed in three independent experiments in triplicate, and the data presented are the mean of the values \pm SD. The growth curves were performed in two independent experiments and the data presented are the mean of the values.

In order to test the attachment of the PS to the cell wall (Section 3.4), *Pf* 2289 was grown on UF-lac at 30 °C in calibrated tubes. After about 6 days of growth, samples were taken and centrifuged at 7000 or 12,000 or 16,000 \times g (15 min, 4 °C), before being dried as described above.

2.6. Sonication of *Pf* 2289 bacterial cultures

For specific experiments (mentioned in the text), the *Pf* culture was treated by sonication (Q700; Q-sonica, Newton, CT, USA) to dissociate PS from the bacterial cells. For 100 ml of culture, sonication was performed using a microtip, on ice, with pulsing at 10 s on/10 s off, to prevent warming of the culture. Energy accumulation was monitored during sonication, and the total energy input was about 2 kJoules for 100 ml. In these sonication conditions, the viability, measured by enumeration of bacteria before and after sonication, was not affected (data not shown).

2.7. Atomic force microscopy (AFM)

Cultures of *Pf* 2289 and *Pf* 456 were grown in UF-lac for 72 h at 30 °C and then centrifuged (7000 \times g, 5 min, room temperature). The pellet was resuspended in HEPES-Na buffer (2 mM 4-(2-hydroxyethyl)-1-piperazineethanesulfonic acid, 50 mM NaCl, pH 6.8) and washed three times by repeated centrifugation and dispersion in fresh buffer.

Immobilization of the bacteria was performed on silanized Histo-bond glass slides (Marienfeld Superior, Lauda-Köningshofen, Germany). First, one volume of 0.4M EDC (N-ethyl-N'-(dimethylaminopropyl)carbodiimide), one volume of 0.1M NHS (N-hydroxysuccinimide) and two volumes of concanavalin-A (Con-A, Sigma Aldrich, 0.3 g l⁻¹ in HEPES-Na buffer) were extemporaneously mixed, deposited on the Histo-bond

slide, and then left to incubate for 20 min at room temperature to allow chemical grafting of the Con-A onto the glass slide by carbodiimide chemistry. The Con-A-coated slides were then extensively rinsed with buffer, prior to deposition of the washed bacterial suspension, diluted two-fold with HEPES-Na-Ca-Mn buffer (2 mM HEPES, 50 mM NaCl, 1 mM CaCl₂, 1 mM MnCl₂, pH 6.8). After 1 h incubation at room temperature, the slides were extensively rinsed with HEPES-Na-Ca-Mn buffer and AFM force mapping was then performed in the same medium. Noteworthy, no proper immobilization of the bacteria could be obtained with simpler methods like physical immobilization in track-etched polycarbonate membranes or chemical immobilization onto polylysine, polyethyleneimine or silane-coated slides, even with carbodiimide chemistry (not shown). It should also be noted that the bare silicon tips of MSNL probes (Bruker Nano Surfaces, Santa Barbara, CA, USA) failed to adhere to the bacterial surface. To circumvent this issue, Con-A was also grafted onto the AFM probes, using a method adapted from Gruber's group (<http://www.jku.at/biophysics/content>) (Francius et al., 2009). Briefly, MSNL probes were first cleaned using UV/O₃ treatment and then immersed in 5% v/v APTES (3-aminopropyl-trimethoxysilane) in absolute ethanol, for 1 h at room temperature. After rinsing in absolute ethanol followed by chloroform, the silanized probes were immersed in chloroform with an 18-polyethylene-glycol crosslinker (acetal-PEG18-NHS crosslinker, 6 nm in length; Johannes Kepler University, Linz, Austria) activated with triethylamine, and left to incubate for 2 h at room temperature in a glass chamber saturated with chloroform to prevent evaporation. The probes were rinsed with chloroform and then dried under an N₂ stream. The PEGylated probes were further immersed in 1% w/v citric acid to convert the acetal into reactive aldehyde, rinsed with Milli-Q water, and then immediately immersed in a droplet of 0.3 g l⁻¹ Con-A in HEPES-Na buffer, to which sodium cyanoborohydride was added extemporaneously. Finally, the unreacted aldehydes were passivated using 1M ethanolamine, pH 8.0. The Con-A grafted MSNL probes were then rinsed with HEPES-Na buffer and stored for up to 5 days in buffer at 5 °C.

Force mapping was performed using an MFP-3D Bio atomic force microscope (Oxford Instruments, Asylum Research, Santa Barbara, CA, USA). The grafted MSNL probes (nominal spring constant $k \sim 0.03$ or 0.1 N m⁻¹) were calibrated extemporaneously against glass and in HEPES-Na buffer, using the thermal noise method. The maps covered $10 \times 10 \mu\text{m}^2$ divided into 64×64 pixels. The maximum contact force was 100 pN, the speed of Z displacement was $2 \mu\text{m s}^{-1}$, and the retraction distance was 1–8 μm , depending on the samples. The temperature inside the droplet was ~ 21 °C. After contact between the Con-A grafted probe and bacteria, retraction of the AFM probe pulled on single molecule(s) that adhered to Con-A, yielding inflection movements of the cantilever and corresponding to negative saw-tooth peaks on the retraction force curves (Francius et al., 2008; Marszalek and Dufrene, 2012). These peaks indicate rupture of the probe/polymer interactions or unfolding/stretching of the molecule upon extension, up to the final separation of the probe and bacteria. In these experiments, the adhesion is regarded as the maximum rupture force recorded along a retraction curve. Furthermore, the elastic behavior of flexible macromolecules such as polysaccharides can be described using the extended freely-jointed chain (FJC+) model, which considers the polysaccharide to be a series of rigid and independently oriented segments (the Kuhn segments), loosely attached end-to-end in series (Marszalek and Dufrene, 2012; Burgain et al., 2014). The Kuhn segments have a characteristic length l_k , dependent on the chain's stiffness, and the linearly extended form of the chain yields the contour length L_c , since $L_c = nl_k$ where n is the number of segments. In the FJC + model, the pulling force F is expressed as a function of the pulling (or separation) distance x as follows:

$$x(F) = L_c [\coth(Fl_k / k_B T) - k_B T / Fl_k] [1 + nF / k_s L_c]$$

where k_s is the elasticity of one Kuhn segment, k_B the Boltzmann

constant and T the temperature. Three independent observations were conducted for each type of bacteria *Pf* 2289, *Pf* 456 or sonicated *Pf* 2289 using different slides and different AFM probes for each observation. Two different cultures were used for *Pf* 2289 and *Pf* 456, two maps were obtained with one culture, and one map was obtained with a second culture. To ensure that no contamination occurred, control slides were mapped before and/or after the bacteria slides.

Finally, the immobilized bacteria were rinsed with Milli-Q water and the slides were placed in a dessicator to dry. The samples were then imaged by AFM in air and in contact mode, using bare MSNL probes (nominal spring constant $k \sim 0.03$ N m⁻¹), scan rates of $5\text{--}20 \mu\text{m s}^{-1}$ and load below 1 nN. Two independent observations were conducted for each type of bacteria.

2.8. Adhesion to abiotic surface assays

The measurement of biofilm formation by *Pf* strains was based on a method previously described by O'Toole (2011) with minor modifications. For each assay, 1 ml of a 24 h culture of *Pf* grown on YEL or UF-lac was diluted in the same fresh medium (1% v/v), and 200 μl were added to 96-well polystyrene tissue culture-treated plates or 96-well polystyrene untreated plates (CytoOne). Untreated polystyrene is hydrophobic, whereas it is made hydrophilic by treatment, usually by oxygen plasma discharge. Plates were incubated anaerobically without agitation at 30 °C for 72 h. Twenty-four replicates for each strain and each culture medium were used for each assay and three independent experiments were conducted. After incubation, the biofilm was stained as follows. The plates were turned over to shake out the liquid and were then gently washed by immersion in distilled water and turned over again to empty the liquid (four times). After drying at room temperature, the wells were filled with 200 μl of 0.1% (w/v) crystal violet in water, and were allowed to stand for 15 min at room temperature. Unbound crystal violet was washed off with distilled water, and the plates were left to dry at room temperature. Cell-bound crystal violet was then dissolved in 30% (v/v) acetic acid for 15 min. The absorbance (A_{550}) was then measured. The analyses were repeated with two independent assays (12 replicates for each assay). To give an indication of the statistical significance of the results, p -values were determined with a bilateral t -test, comparing the two strains.

3. Results & discussion

3.1. *Pf* 2289: a strain with an original morphology

Propionibacterium freudenreichii are described as pleiomorphic bacillae (coccoid to rod shape), with dimensions of $1.0\text{--}1.5 \mu\text{m} \times 0.5\text{--}0.8 \mu\text{m}$ and forming round and regular creamy-white colonies on YEL agar plates (Cummins and Johnson, 1986). The strain *Pf* 2289, which was originally isolated from Morbier cheese, retained our attention because it exhibited an unclassical phenotype. On plates, YEL agar or UF-lac agar, the *Pf* 2289 colonies looked like molar teeth (Fig. 1a). They presented an irregular circumference, their shape was not convex and their sizes were small (1.2–2.4 mm in diameter). The color, however, was typical of the species. The colonies were not ropy and no strands could be formed by extension with a loop. In UF-lac liquid culture, *Pf* 2289 also presented an atypical phenotype. During the exponential growth phase (between 0 and 48 h) the culture was homogeneous, with non-aggregative cells in the medium. During the stationary growth phase (after $\cong 48$ h of growth) the cells became aggregated, and cells embedded in a thick slimy matrix coexisted with free cells, as confirmed by microscopic observation (Fig. 1b). When the stationary-growth-phase culture was centrifuged, the slimy matrix prevented the bacteria from forming a tight pellet. On the contrary, the centrifuged bacteria formed a soft and bulky pellet (Fig. 1c), which was very difficult to resuspend in liquid medium using standard procedures (vortex or vortex with glass beads). When *Pf* 2289 was cultured on YEL liquid medium, the culture

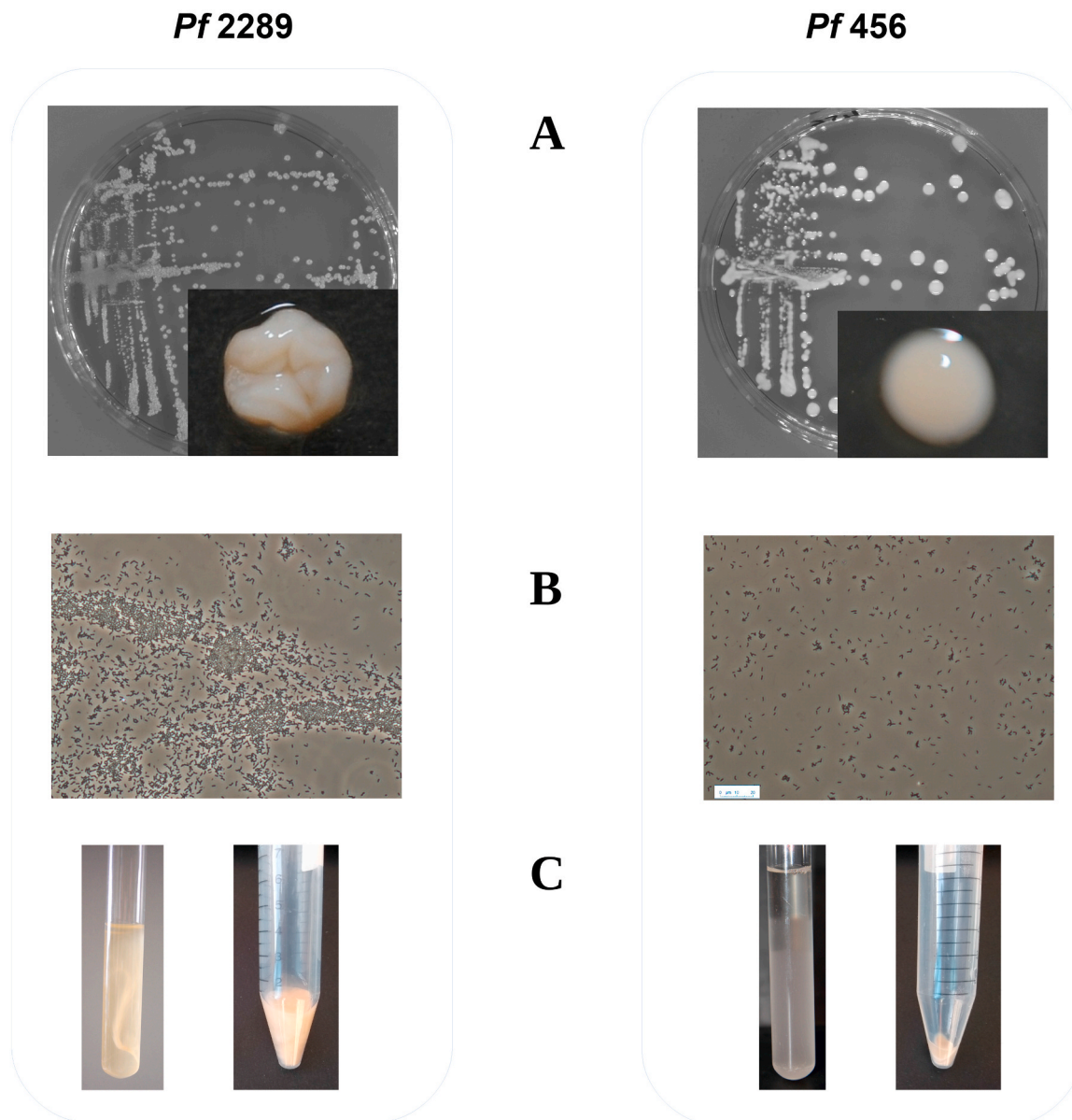


Fig. 1. Morphotypes of the unclassical strain *Propionibacterium freudenreichii* CIRM BIA 2289 (left column) or its derivative CIRM BIA 456 that presents characteristics typical of the species (right column). (A) Observation of colonies after growth in YEL or UF-lac agar plates. (B) Microscopic observation of the two strains grown to stationary phase in a liquid UF-lac medium. (C) Macroscopic observation of cultures of the two strains in liquid UF-lac medium (stationary growth phase) and of the corresponding pellet obtained after cultures centrifugation (7000×g, 15 min, room temperature) and removal of the supernatant.

presented a phenotype similar to the classical one observed for *Pf* strains, no slimy matrix was observed regardless of the growth phase, and the cells were not aggregated (not shown). Viscous liquid cultures are among the first criteria taken into account when looking for PS-producing bacteria. The aspect of the slimy matrix produced by *Pf* 2289 when grown on liquid UF-lac medium thus points towards the production of PS, even if the clones on agar medium were not ropy.

In this case, *Pf* 2289 produced the abundant slimy matrix when grown on liquid UF-lac, but not on YEL medium. This indicates that PS production is medium-dependent, as has often been described in other bacteria, with the carbon source as a determinant parameter (Polak-Berecka et al., 2015; Fraunhofer et al., 2018). In order to determine the influence of the carbon source on PS production of *Pf* 2289, the strain was cultured in a liquid YE-lactose or YEL-lactose media. No production of slimy matrix was observed within 96 h of culture. This indicates that the carbon source is perhaps necessary but not sufficient to restore the PS production observed with UF-lac medium. We cannot however

exclude the possibility that an unknown YEL component prevented the production of PS by *Pf* 2289 cells in liquid cultures. The differences observed in the two mediums, UF-lac or YEL, reveal that the phenotype is dependent on the medium and that slime production is triggered by UF-lac. Finally, on plates, the “molar-shaped” morphotype of *Pf* 2289 is observed after growth on YEL agar or UF-lac agar, as well as on YE-lactose agar and YEL-lactose agar (not shown), suggesting that in solid medium, PS is synthesized regardless of the medium.

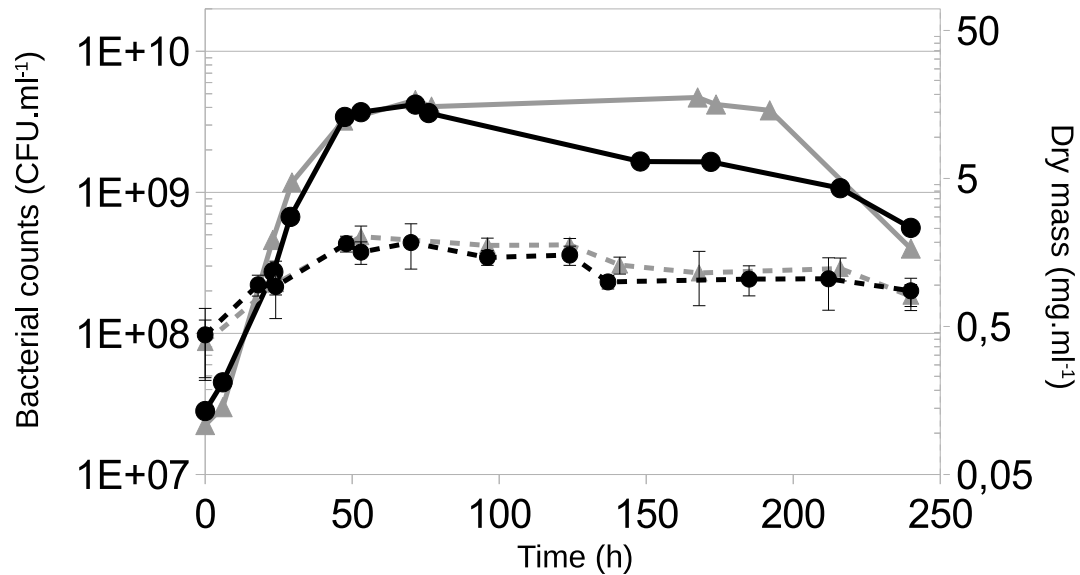
3.2. *Pf* 456: a derivative that has irreversibly lost the molar-shaped morphotype

Interestingly, when plating *Pf* 2289 on YEL agar plates, a minority morphotype was observed in addition to the molar-shaped morphotype. This morphotype was observed at a frequency of 4% of the colonies (over about 1000 colonies). These minority colonies presented typical characteristics of the *Pf* species, with a smooth and brilliant surface and

a regular circumference (Fig. 1a). One clone of this morphotype was isolated. After re-isolation on YEL agar plate, the strain was considered to be pure and was referred to as CIRM BIA 456 (abbreviated as *Pf* 456). The morphotype of *Pf* 456 on UF-lac agar plates was the same as on YEL agar plates, i.e., regular colonies (Fig. 1a). When cultured in UF-lac liquid medium, unlike *Pf* 2289, *Pf* 456 did not produce the slimy matrix. When centrifuged, the pelleted cells presented a small pellet

(Fig. 1c), which was easy to resuspend in liquid medium. Whether in liquid culture or on YEL agar plates, *Pf* 456 thus presented the typical phenotype of the species described above. On the basis of the differences between morphotypes and the slimy matrix production between *Pf* 2289 and *Pf* 456, we hypothesized that *Pf* 2289 is a distinctive strain that has the ability to produce a PS, whereas *Pf* 456 has lost the ability, with the consequence of the loss of the “molar-shaped” morphotype of its

A – YEL



B – UF-lac

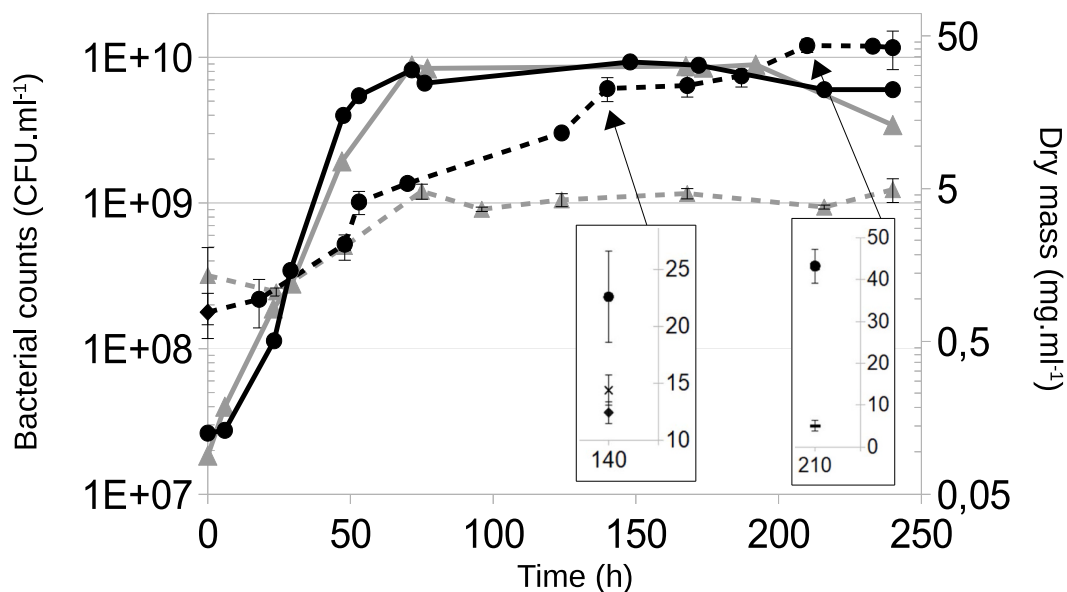


Fig. 2. Growth of *Propionibacterium freudenreichii* CIRM BIA 2289 or its derivative CIRM BIA 456. The strains *Pf* 2289 (black lines) and *Pf* 456 (grey lines) were grown on (A) YEL or (B) UF-lac medium at 30 °C. Left axis & solid lines: the growth was followed by bacterial counts. From 24h, the cultures were treated by sonication before counting. Right axis & dotted lines: the growth was followed by dry mass measurement of the pelleted bacteria. The strains were grown in calibrated tubes and at different times the cultures were centrifugated (7000×g, 15 min, 4 °C), and after removal of supernatant, the pellets were dried before being weighed. In inclusion in (B): at 140 h, two centrifugation speeds were tested in parallel: (x) 12,000×g and (◆)16,000×g; at 210 h, strain *Pf* 2289 was sonicated before dry mass determination: (●) not sonicated cells, (-) sonicated cells.

colonies. Indeed, numerous studies have described morphotypic variations associated with the synthesis of PS by bacteria, associated or not with the production of ropy or slimy material. For example, the probiotic strain CNCM-I-3699 of *Lactobacillus farciminis* presented two morphotypes on plating: rough or smooth. The smooth morphotype, ropy on plating, was shown to produce greater quantities of capsular PS, compared to the rough one. The rough morphotype was shown to aggregate and sediment, whereas the smooth one did not (Tareb et al., 2015, 2017). In *Lactobacillus johnsonii*, the strain FI9785 and its spontaneous variant presented different colony morphotypes with different surface properties that were linked to the production of a PS synthesis (Horn et al., 2013).

The reversibility of the *Pf* 456 minority morphotype towards the parental molar-shaped morphotype was tested by plating a liquid culture of *Pf* 456 on YEL agar plates. No clone with the parental molar-shaped morphotype was detected (over about 5000 colonies), indicating that the loss of the molar-shaped morphology is not reversible. In addition, we tested the stability of the minority morphotype in liquid medium by sub-culturing *Pf* 456 in UF-lac. After ten successive sub-cultures, no change of phenotype was observed, and the *Pf* 456 cultures were unable to restore the slimy matrix production. In conclusion, the original morphotype *Pf* 2289 isolated from Morbier cheese exhibits medium-specific production of a slimy matrix, whose loss is irreversible and yields a morphotype closer to that of typical *Pf*.

3.3. PS production by *Pf* 2289

We thus investigated the production of PS by both strain *Pf* 2289 and its derivative *Pf* 456 via an indirect method: we measured the microbial biomass, expressed as dry mass of pelleted cells, during growth. In parallel, we measured bacterial counts. The time courses of growth and biomass in UF-lac and YEL are presented in Fig. 2. In YEL (Fig. 2a), *Pf* 2289 and *Pf* 456 presented similar growth curves with a generation time of 6.5 h during the exponential growth phase. The maximal populations measured were also close: 3.70×10^9 and 4.51×10^9 CFU ml⁻¹ for *Pf* 2289 and *Pf* 456, respectively. During the stationary growth phase, the population decreased for both strains and dropped to 5.6×10^8 and 4.0×10^8 CFU ml⁻¹ after 240 h of incubation for *Pf* 2289 and *Pf* 456, respectively. The biomass increased for both strains during the exponential growth phase and a maximal biomass was measured when the bacterial counts were the highest, i.e., after 48 h of growth for *Pf* 2289 with a biomass of 1.8 mg ml⁻¹, and after 53 h for *Pf* 456 in YEL with a biomass of 1.9 mg ml⁻¹. After 240 h of incubation for *Pf* 456, the bacterial counts dropped to 4.0×10^8 CFU ml⁻¹, whereas the biomass remained stable, suggesting that bacteria are in a viable but not cultivable state. In UF-lac medium, *Pf* 456 presented a behavior quite similar to that observed in YEL (Fig. 2b). However, the generation time was longer (7.3h), and the maximal population higher (8.8×10^9 CFU ml⁻¹, reached after 71 h of incubation), dropping to 3.4×10^9 CFU ml⁻¹ after 240 h of incubation. The maximal biomass obtained was 4.6 mg ml⁻¹, when the counts were the highest. For the strain *Pf* 2289 in UF-lac, the growth curve estimated by bacterial counts presented the same behavior as *Pf* 456, but with a generation time of 5.8 h and a maximal population of 8×10^9 CFU ml⁻¹. However, the biomass curve increased during the exponential growth phase (0–48 h), as well as during the stationary growth phase, reaching a biomass of 43 mg ml⁻¹ after 210 h of growth and remaining stable until the end of the kinetics. When calculating the ratio of dry mass (in mg) for 10⁹ bacteria at the points of highest biomass, we obtained values of 7.16 for *Pf* 2289 in UF-lac, whereas we found ratios of 0.46 for *Pf* 456. In YEL, we obtained ratios of 0.45 and 0.42 mg/for 10⁹ bacteria for *Pf* 2289 and *Pf* 456, respectively. The differences in biomass measured for *Pf* 2289 after growth in YEL and UF-lac together with the biomass, which are similar between *Pf* 2289 and *Pf* 456 when grown on YEL, indicate that PS production takes place only in UF-lac medium. This is in accordance with the appearance of the slimy matrix observed for this strain. Furthermore, PS production takes place

during the late stationary growth phase when the cells are still metabolically active but no longer divide. Therefore, for *Pf* 2289, the PS production constitutes the main part of the biomass of pelleted cells.

3.4. PS produced by *Pf* 2289 is loosely bound

We then investigated the attachment of the PS produced by *Pf* 2289 cells in UF-lac medium. When we measured the dry mass of pelleted cells (see above), the PS were collected at the same time as the bacteria during the centrifugation step, indicating that the PS remained bound to the bacteria. With a *Pf* 2289 culture of 140 h in UF-lac, we tested two centrifugation speeds: 12,000×g and 16,000×g. In these conditions, the dry mass of pelleted cells was 14.4 ± 1.3 and 12.4 ± 0.9 mg ml⁻¹, respectively, whereas it was 20.8 ± 3 mg ml⁻¹ with a centrifugation at 7000×g. The centrifugation at high speed thus allowed the PS to detach from the cells, as has already been observed for PS of different species (Brown and Lester, 1980; Zhao et al., 2015). Finally, we investigated the effect of sonication on the attachment of the PS to the bacteria. After 210 h of UF-lac culture, when the biomass reached its maximum level, a sample of *Pf* 2289 was sonicated before biomass determination. As also observed by Bevilacqua et al. (2019) on Propionibacteria, and by Joyce et al. (2003) on *Bacillus subtilis*, sonication treatment, when performed at low intensity, does not affect the viability of cells (data not shown). In these conditions, the dry mass of pelleted cells dropped to 5 mg ml⁻¹, whereas it was 43 mg ml⁻¹ without sonication, corresponding to the dry mass of the *Pf* 456 cells. This indicates that sonication allowed PS to be released in the medium. In conclusion, in the present study, the PS produced by *Pf* 2289 is not released into the environment. It is loosely bound to the cell wall instead. Whether it is covalently bound to the cell wall or bound via other compounds remains to be elucidated.

3.5. *Pf* 2289 produces an original PS

The bacterial PS are classified in groups according to their composition and their localization relative to the cell wall. The definition of groups is not homogeneous throughout the literature. PS production by *Pf* is quite well documented, highlighting the fact that it is diverse and strain-dependent, and that not all the strains are able to produce PS. Different types of molecules have been identified in terms of composition and cellular localization, including (i) a PS composed of mannose and glucose that is produced by the strain *Pf* CIP 59.32 (Belgrano et al., 2018); and (ii) a PS composed of D-glucose, D-mannose and D-glucuronic in molar ratios of 2:2:1 that is produced by the strains *Pf* 109 and *Pf* 111 (Dobrucowska et al., 2008). These two heteropolysaccharides have been shown to be released in the culture medium. Using a specific immunoagglutination test, 35% of the 68 strains of *Pf* tested were shown to produce a bound cell wall PS composed of (1 → 3,1 → 2)-β-D-glucan (Deutsch et al., 2008, 2010). This glucan exhibits a comb-like structure of glucose units branched 1 → 2 to the backbone 1 → 3 glucose chain (Adeyeye et al., 1988; McIntosh et al., 2005). The production of this cell wall glucan was also observed in two other strains of *Pf* (out of ten tested) by Tinzl-Malang et al. (2015). In the well-studied probiotic strain *Pf* JS (Nordmark et al., 2005), a PS with the same composition was identified, but in this case, the molecule was recovered from the culture supernatant after centrifugation of cells. This indicates that either all the PS or at least a part of it is released in the culture medium. As a first approach, we tested whether or not the PS produced by *Pf* 2289 could be the β-D-glucan described above. For that purpose, the strains were subjected to an agglutination test, performed with the antiserum specific to (1 → 3,1 → 2)-β-D-glucan. The strain *Pf* CIRM-BIA 1^T was used as a positive control since it is known to produce surface β-D-glucan (Deutsch et al., 2012); a strong agglutination of bacteria is observed in the presence of the antiserum regardless of the culture medium used for the growth (UF-lac (Fig. 3) or YEL (not shown)). The strain *Pf* 456 presented no agglutination in the presence of the antiserum, whether in UF-lac (Fig. 3) or in YEL (not shown). The results were the same regardless of

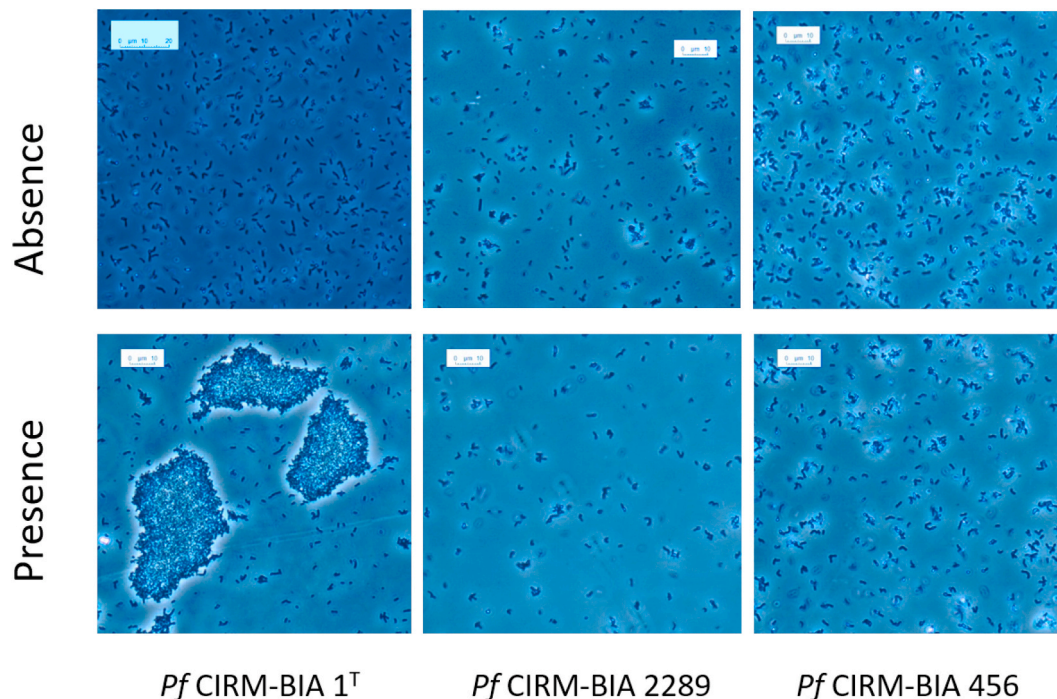


Fig. 3. Immunoprecipitation test performed with an (1 → 3,1 → 2)-β-D-glucan-specific antiserum on 3 strains of *Propiobacterium freudenreichii*: CIRM BIA 1^T, used as positive control, and CIRM BIA 2289 and its derivative CIRM BIA 456. The test was performed with cultures grown in YEL medium, and the images presents the microscopic observations done in absence (top images) or in presence (bottom images) of antiserum.

the growth phase tested (data not shown). The strain *Pf* 2289 was first tested during the exponential growth phase in UF-lac, and no agglutination was observed (Fig. 3). The test performed with *Pf* 2289 after growth in YEL was also negative (data not shown). When the test was performed with cells during the stationary growth phase, the result was less obvious since the slimy matrix produced and embedding the cells made it impossible to clearly see any immunoprecipitation. Nevertheless, no agglutination was observed in the regions with free cells detached from the slimy matrix (data not shown), indicating that no β-D-glucan is produced. All together, these tests indicate that neither *Pf* 2289 nor *Pf* 456 produced the (1 → 3,1 → 2)-β-D-glucan frequently encountered in *Pf* strains, regardless of the growth phase and the medium used.

3.6. Surface properties of *Pf* 2289 and its derivative: analysis by AFM

The surface properties associated with PS production were investigated by AFM analysis. AFM deflection images of *Pf* 2289 and its derivative *Pf* 456 provided details of the surface of their respective cell walls. Strain *Pf* 2289 clearly showed a rough surface, with the appearance of entangled filaments spread over the whole surface of the bacteria (Fig. 4a). Meanwhile, *Pf* 456 exhibited a smooth surface, even showing traces of former septa. Respective rugosities of 8.7 and 6 nm were calculated on 300 × 300 nm² samples of the AFM images, where planar surfaces could be found on the bacteria (N = 5). The contours of *Pf* 456 individuals were sharp, while those of *Pf* 2289 were blurred as a result of PS production. Fig. 4b shows that both *Pf* 2289 and *Pf* 456 were successfully immobilized onto Con-A coated glass slides in the presence of Mn and Ca ions. This indicated the presence of D-glucose and/or D-mannose exposed at the surface of both bacteria, either on glycosylated proteins and/or most likely in the protruding PS of the cell wall. The topography force maps showed that some loose protruding material seemed to be attached to the bacteria, especially in *Pf* 2289 (blue arrows in Fig. 4b). This was interpreted as parts of PS synthesized by this strain, which formed a slimy matrix in liquid UF-lac culture. Some individuals appeared devoid of this material, possibly as a result of an earlier growth

stage and/or of the repeated centrifugation process used to wash the cultures. At higher rates, centrifugation can remove pili (Tripathi et al., 2012) and detach polysaccharides (Brown and Lester, 1980; Zhao et al., 2015). The corresponding adhesion (or maximum rupture) force maps provide the maximum adhesion force value that can be locally measured locally on retracting the AFM probe after contact with the sample on each pixel of the map (Fig. 4b). Examples of typical retraction curves, taken at random where adhesion was significant, are provided in Fig. 4c and 4d shows how the FJC + model is fitted onto the curves (left panel, red traces). Series of rupture peaks are interpreted as resulting from the elongation of polymer(s) picked up by the Con-A-grafted AFM probe upon contact with the bacterial surface through the successive stretching of polymer loops in single molecules and the detachment of the polymer(s) as pulling by the AFM probe exceeds their maximum length (Francius et al., 2009, 2008). The analysis of the sawtooth-patterned retraction force curves revealed molecular elongations occurring up to 6000 nm and 600 nm for *Pf*2289 and *Pf*456, respectively. Adhesion force maps clearly showed that greater adhesion was observed for both strains on and around the loose material attached to the bacteria, as well as in the vicinity of the bacteria, indicating the correspondence between adhesion and the presence of the bacterial PS (Formosa-Dague et al., 2016). Adhesion values were greater in *Pf* 2289 than in *Pf* 456, with significantly more frequent values over 100 pN and even 200 pN in *Pf* 2289 (Fig. 4b, red and yellow pixels). These forces are in the range of those found in similar studies that also investigated bacterial adhesion by capsular polysaccharides using lectin-coated probes (Francius et al., 2008; Fahs et al., 2014; Wang et al., 2015). The greater adhesion of *Pf* 2289 is also visible in the rupture force histograms, which collects individual force values of all the rupture peaks in the 64 × 64 force curves in a map. Fig. 4d, related to the statistical analysis of whole retraction force curves, shows that adhesive events (rupture forces) greater than 200 pN are more frequent in *Pf* 2289 than in *Pf* 456. In the absence of bacteria, the adhesion force between the AFM probe and the Con-A-coated slides is typically ~25 pN or lower, in the presence of Ca and Mn (not shown). Furthermore, the maximum elongation lengths observed on pulling polymers of the cellular PS were significantly

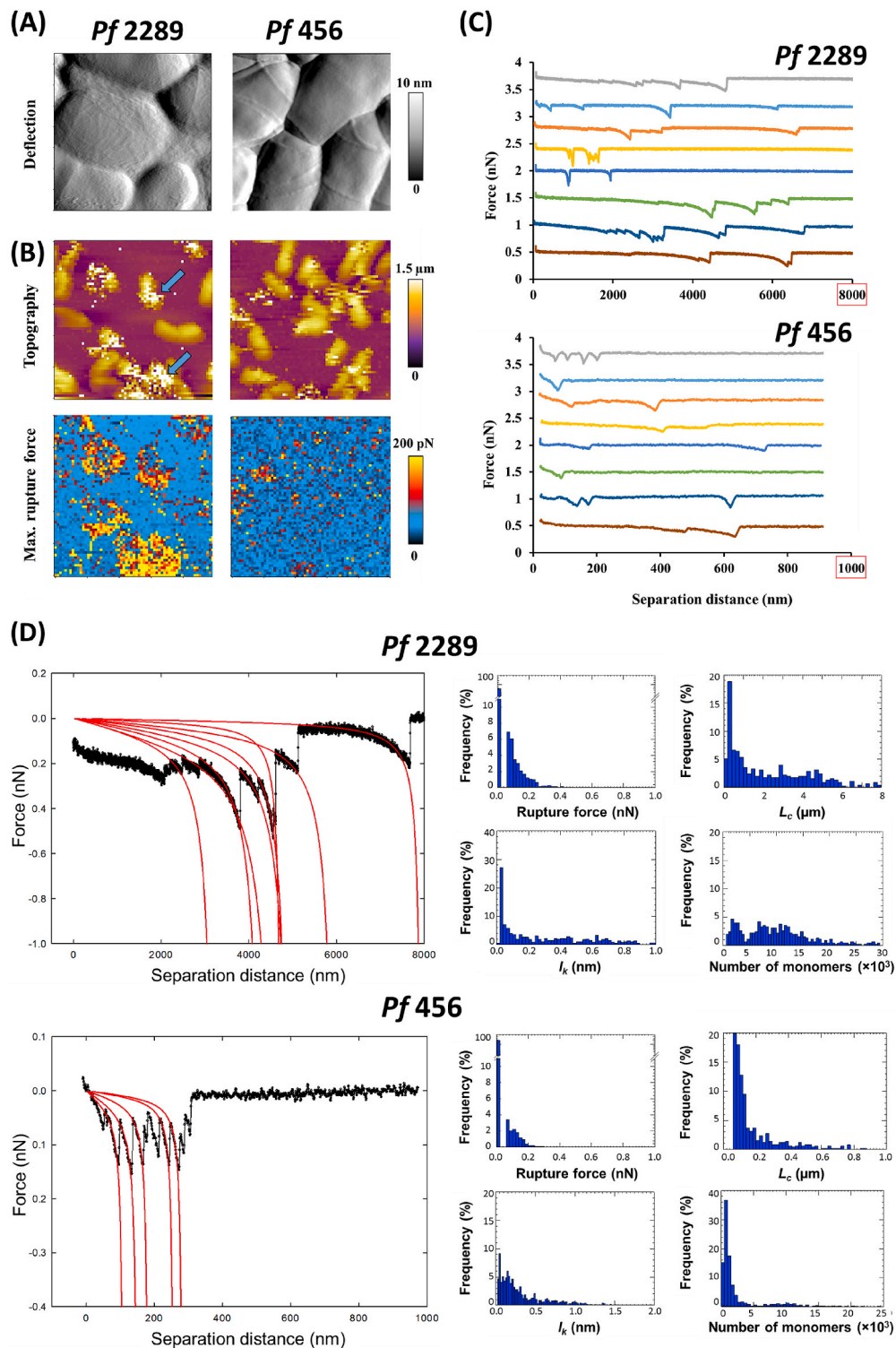


Fig. 4. Atomic force microscopy comparison between *Propionibacterium freudenreichii* CIRM BIA 2289 and its derivative CIRM BIA 456. (A) $1.5 \times 1.5 \mu\text{m}^2$ deflection images of Pf 2289 (left) and Pf 456 (right), taken in air after deposition of the washed culture onto mica then dehydration, showing details of the bacterial surface. (B) $10 \times 10 \mu\text{m}^2$ (64×64 pixels) force maps images of washed cultures of Pf 2289 (left) and Pf 456 (right), taken at $\sim 21^\circ\text{C}$ in HEPES-Na-Ca-Mn buffer at pH 6.8. The top images show the topography of the sample, evidencing the presence of immobilized bacteria, while bottom images show the corresponding adhesion map (maximum rupture force map) recorded over the same area. (C) Typical retraction force curves recorded over “warm” (red to yellow) pixels of the Pf 2289 and Pf 456 adhesion force maps, taken at random, evidencing the elongation length of wall components adhering to the grafted AFM probe. Individual force curves are shifted along the Y-axis for clarity. Mind the different scales in X-axis. (D) Application of the freely jointed chain + (FJC+) model to the retraction force curves. Examples of the fit are shown in red for Pf 2289 (up) and Pf 456 (bottom) in the left panel, while the right panel provides the output histograms of the maximum rupture force of the last adhesive event (top row), the contour length L_c of the last adhesive event (top right), the Kuhn length l_k (bottom left) and the estimated number of monomers per chain (bottom right) calculated using the FJC + model over the 64×64 force curves of the AFM force maps. (For interpretation of the references to color in this figure legend, the reader is referred to the Web version of this article.)

greater for *Pf* 2289 than for *Pf* 456, with distances of up to 7 μm for the former and less than 1 μm for the latter (Fig. 4c). It is worth noting that when significant amounts of slime were present on AFM slides of *Pf* 2289, immobilization was too loose to allow a full force map to be recorded, but lengths over 10 μm could be occasionally observed (not shown). This is also well illustrated by the calculation of the contour length L_c of the pulled polymers (Fig. 4d). Noteworthy, while the FJC + model considers the unfolding and extension of a single molecule, it is possible that the sawtooth patterns of the retraction force curves also arose from simultaneous stretching events of several molecules picked up by the AFM probe upon contact with the bacterial PS. In this case, only the very last unfolding peak is undoubtedly that of a single molecule, as the last one to detach. To circumvent this issue, the rupture force and the contour length L_c of the polymer were calculated using only the last adhesive event over all the retraction curves. No significant difference was found depending on whether only the last peak (Fig. 4d) or all peaks (not shown) was/were fitted by the FJC + model, which supported the single-molecule hypothesis altogether. Application of the FJC + model furthermore yielded Kuhn's lengths l_k of putative monomers of less than 1 nm for both strains (with the occurrence of some higher values in *Pf* 2289), illustrating high molecular flexibility of the

bacterial PS. Moreover, it should be noted that Kuhn's length l_k distributions appeared to be more homogeneous for *Pf* 456 with a pseudo monomodal shape spanning 0–500 pm, than for *Pf* 2289. For the latter, Kuhn's length values are rather randomly distributed over a range of 50–1000 pm but with less than 30% under 50 pm. Hence, the pulled molecules would correspond to long chains of up to 30,000 monomer segments in *Pf* 2289 vs. shorter ones of about 5000 in *Pf* 456. Regarding these conformational parameters, it can be observed that PS produced by *Pf* 2289 are more flexible, 5–10 times longer and more heterogeneous than those detected on *Pf* 456. Using the same method, EPS stretched out of biofilms of *Pseudomonas fluorescens* were ~20,000 segments long (Fahs et al., 2014). In places where *Pf* 2289 bacteria was immobilized in the form of slimy clusters, elongation distances exceeded the possible maximum retraction distance of the Z piezo of the AFM (15 μm) to the extent that force mapping could not be performed (not shown). In conclusion, AFM investigation of the surface of living or dried bacteria clearly showed that *Pf* 456 exhibited a smoother surface, less and shorter cell wall polymers and significantly lower adhesion to Con-A than its *Pf* 2289 parental counterpart. As regarding the AFM-tip functionalization with Con-A and results obtained from theoretical fitting, we can assume that the PS produced by the bacteria should be mostly enriched in

Pf 2289 + sonication

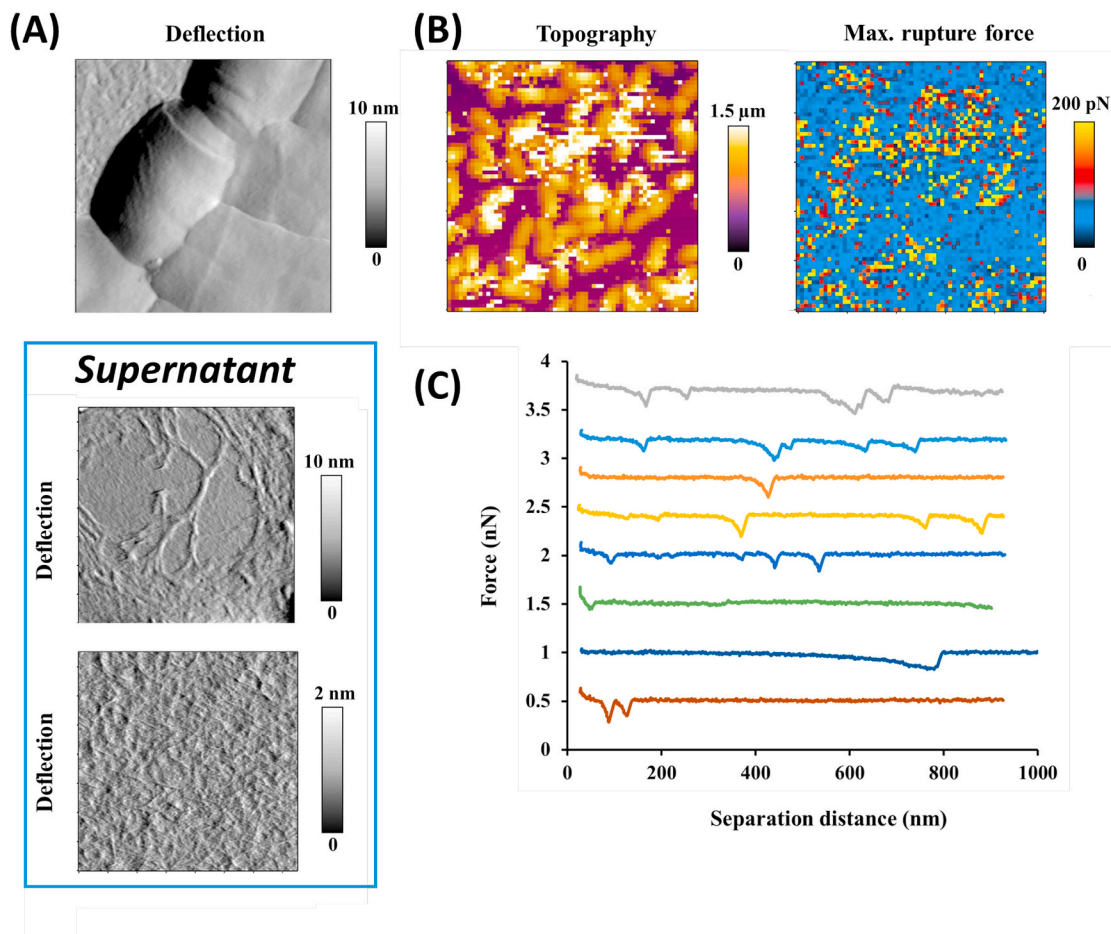


Fig. 5. Atomic force microscopy observation of *Propionibacterium freudenreichii* CIRM BIA 2289 after sonication and washing of the stationary phase culture in UF-lac medium. (A) $1.5 \times 1.5 \mu\text{m}^2$ deflection image of the bacteria taken in air. (B) $10 \times 10 \mu\text{m}^2$ (64×64 pixels) topography and maximum rupture force (adhesion) maps images of the washed culture of sonicated *Pf* 2289, taken at $\sim 21^\circ\text{C}$ in HEPES-Na-Ca-Mn buffer at pH 6.8. (C) Typical retraction force curves recorded over “warm” pixels of the maximum rupture force map, evidencing the elongation length of wall components adhering to the grafted AFM probe. Individual force curves are shifted along the Y-axis for clarity. The inserted blue-framed panel shows deflection images of the material found into the supernatant of the sonicated *Pf* 2289 culture, after deposition onto glass slide and dessication. (For interpretation of the references to color in this figure legend, the reader is referred to the Web version of this article.)

mannose and/or glucose (Francius et al., 2008).

As a complement, *Pf* 2289 was cultured in UF-lac medium and then sonicated prior to washing and immobilization onto Con-A glass slides, like for the *Pf* 2289 and *Pf* 456 cultures. AFM deflection images showed that the appearance of sonicated *Pf* 2289 was close to that of *Pf* 456, i.e., they exhibited a soft surface devoid of filaments or blurry material (Fig. 5a).

Topography and adhesion force maps in HEPES-Na-Ca-Mn buffer showed that sonicated *Pf* 2289 bacteria still exhibited loose material on some individuals, but the frequency and the magnitude of the adhesion events were reduced compared to the unsonicated samples (Fig. 5B vs. Fig. 4B). The retraction force curves indicated much shorter PS molecules after sonication, with an extension of within 1 μm instead of 7 μm (Fig. 5c vs. Fig. 4c).

When the *Pf* 2289 culture was washed multiple times at 7000 \times g, 5 min in Milli-Q water and then sonicated, it was possible to recover the supernatant of sonicated washed *Pf* 2289 after a final high-speed centrifugation (16,000 \times g, 10 min). Droplets of the supernatant were left to dry on glass slides in a dessicator and then imaged by AFM in the air in the same conditions as the dried bacteria. A thick material was visible on the slides, and close investigation with AFM showed that filamentous or stranded organization could be observed (Fig. 5, blue-framed inset). In conclusion, AFM investigation confirmed that sonication removed a large proportion of the attached PS of *Pf* 2289 cells, and that these PS could be recovered by washing prior to sonication.

3.7. Surface properties of *Pf* 2289 and its derivative: biofilm formation on abiotic surfaces

In order to understand the impact of the presence of the cell wall PS on the surface properties of the bacteria, we investigated the ability of *Pf* 2289 and its derivative to form biofilms on abiotic surfaces, i.e., polystyrene deep-well-plates, treated or not for cellular culture (Fig. 6). Using plates treated for cellular culture (Fig. 6a), the strain *Pf* 2289 presented a low biofilm formation ability, regardless of the culture medium used for the growth (YEL or UF-lac), with $A_{550} < 0.2$ (no significant differences between the two media). On the contrary, the strain *Pf* 456 presented moderate biofilm formation ability, with an A_{550} of 0.53 and 1.22, after growth on YEL and UF-lac, respectively. Using non-treated polystyrene, the ability of strain *Pf* 2289 to form biofilm was still very low, regardless of the growth medium used ($A_{550} < 0.1$). This is also coherent with observations that *Pf* 2289 barely adhered to polylysine or silanized glass or to plasma-treated silicium (see the AFM section). Interestingly, the strain *Pf* 456 presented a strong ability to form biofilm on polystyrene after growth on either YEL or UF-lac. As observed using treated plates, the biofilms of *Pf* 456 were significantly stronger when cells were grown on UF-lac ($A_{550} = 3.38$) compared to YEL ($A_{550} = 2.85$). Polystyrene is a strongly hydrophobic material and the treatment applied to plates for cellular culture aims to make the polystyrene more hydrophilic. Adhesion to surfaces is one of the crucial steps in biofilm development. The different ability to form biofilms of *Pf* 456 observed between polystyrene microplate types might thus refer to different levels of adhesion of cells according to substrates. *Pf* 456 therefore adheres to the untreated material more than to the treated one, indicating that hydrophobic bonds are established between the polystyrene and some surface component(s) of the bacteria (Pham et al., 2003; Kuyukina et al., 2016). *Pf* 2289 seemed to be able to establish such bonds, indicating that the presence of the PS produced by *Pf* 2289 gives the bacteria specific adhesion properties. It should be noted that this behavior is observed both in YEL, where *Pf* 2289 does not develop a thick slimy matrix, and in UF-lac, where it does so. This confirmed the hypothesis that *Pf* 2289 produces the same PS on YEL and UF-lac, but that the quantity produced upon growth in UF-lac is much greater. In future research, we aim to decipher the biochemistry and structural properties of the PS produced by *Pf* 2289 in order to better account for the adhesion, water-binding, rheology and other potentially valuable

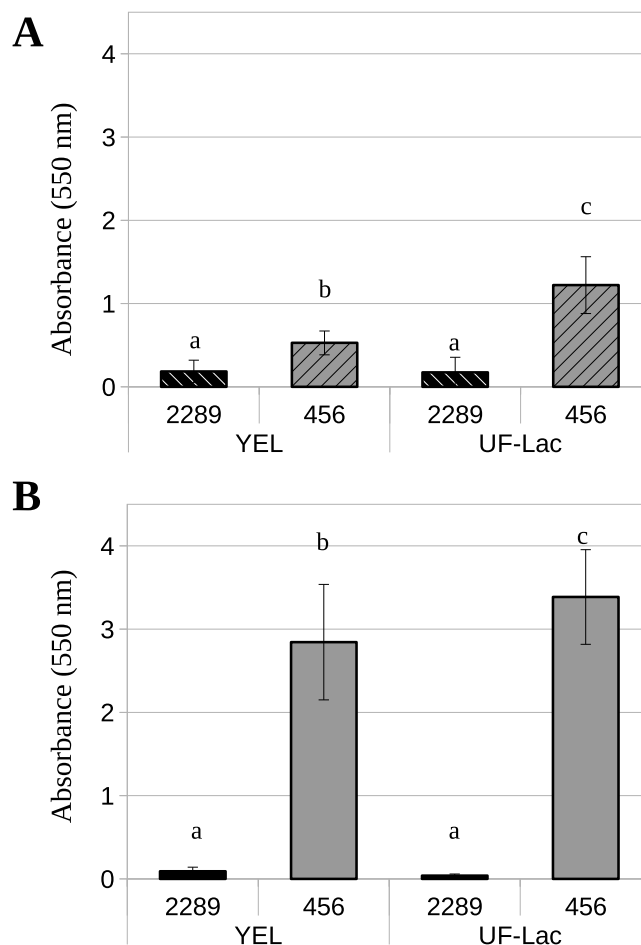


Fig. 6. Biofilm formation on abiotic surface of the PS producing strain *Propionibacterium freudenreichii* CIRM BIA 2289 and its derivative CIRM BIA 456, that lost the ability to produce PS. The strains were inoculated at 1% in YEL or UF-lac medium in polystyrene plates, (A) treated for cellular culture or (B) not treated for cellular culture. After 3 days of incubation at 30 °C, the ability of bacteria to form biofilm was quantified. Data are presented as means \pm SD, and different letters indicate significant difference ($P < 0.05$) amongst strains (student test).

physicochemical properties of *Pf* 2289 and of its PS.

3.8. Conclusion

Our study focused on a strain of *Pf*, *Pf* 2289, which was selected because of its atypical and unstable morphotype. *Pf* 2289 was shown to produce a PS that is bound to the cell wall. The production of this PS is dependent on the medium composition and takes place during the stationary growth phase. The nature of the PS molecule remains to be determined, but the AFM analysis suggested that it probably contains mannose and/or glucose and could reach unusual lengths of over 10 μm . Its complete composition now needs to be elucidated. The presence of this PS molecule gives specific properties to *Pf* 2289, and we observed an inability to adhere to hydrophobic and hydrophilic surfaces. Adhesion to surfaces is a property that needs to be taken into account for specific applications. From this perspective, it would be interesting to compare the adhesion properties of *Pf* 2289 and its variant to biotic surfaces such as epithelial cells. Indeed, adhesion to epithelial cells is one of the criteria evaluated when selecting strains that could settle in the GI tract to exercise their probiotic activity (de Melo Pereira et al., 2018). In a food context, the use *Pf* 2289 that produces a large amount of PS in fermented food products could be useful to improve the texture of the

products, as already observed for a heteropolysaccharide-producing strain of *Pf* in bread (Tinzl-Malang et al., 2015) and in dairy products with different lactic acid bacteria. Finally, the PS production property of *Pf* 2289 is unstable since reversibility sometimes occurs, yielding *Pf* 456, which exhibits properties typical of the species and the loss of the ability to produce the PS. This instability strongly suggests the loss of a modification of the genetic material of *Pf* 2289, and the need for complementary research in the field of genetics to elucidate the metabolic pathway of the production of PS by *Pf* 2289.

Declaration of competing interest

None.

Acknowledgments

STLO's Asylum Research MFP3D-BIO atomic force microscope was funded by the European Union (FEDER), the French Ministry of Education and Research, INRAE, Conseil Général 35 and Rennes Métropole. The authors thank Éric Guédon for his careful proofreading of the manuscript.

References

- Adeyeye, A., Jansson, P.-E., Lindberg, B., Henrichsen, J., 1988. Structural studies of the capsular polysaccharide from *Streptococcus pneumoniae* type 37. *Carbohydr. Res.* 180, 295–299. [https://doi.org/10.1016/0008-6215\(88\)80086-7](https://doi.org/10.1016/0008-6215(88)80086-7).
- Belgrano, F.D.S., Verçoza, B.R.F., Rodrigues, J.C.F., Hatti-Kaul, R., Pereira, N., 2018. EPS production by *Propionibacterium freudenreichii* facilitates its immobilization for propionic acid production. *J. Appl. Microbiol.* 125, 480–489. <https://doi.org/10.1111/jam.13895>.
- Bevilacqua, A., Racioppo, A., Sinigaglia, M., Speranza, B., Campaniello, D., Corbo, M.R., 2019. A low-power ultrasound attenuation improves the stability of biofilm and hydrophobicity of *Propionibacterium freudenreichii* subsp. *freudenreichii* DSM 20271 and *Acidipropionibacterium jensenii* DSM 20535. *Food Microbiol.* 78, 104–109. <https://doi.org/10.1016/j.fm.2018.10.010>.
- Brown, M.J., Lester, J.N., 1980. Comparison of bacterial extracellular polymer extraction methods. *Appl. Environ. Microbiol.* 40, 179–185.
- Burgain, J., Scher, J., Francius, G., Borges, F., Corgneau, M., Revol-Junelles, A.M., Cailliez-Grimal, C., Gaiani, C., 2014. Lactic acid bacteria in dairy food: surface characterization and interactions with food matrix components. *Adv. Colloid Interface Sci.* 213, 21–35. <https://doi.org/10.1016/j.cis.2014.09.005>.
- Chapot Chartier, M.-P., Kulakauskas, S., 2014. Cell wall structure and function in lactic acid bacteria. *Microb. Cell Factories* 13, S9. <https://doi.org/10.1186/1475-2859-13-S1-S9>.
- Cummins, C.S., Johnson, J.L., 1986. Genus I. *Propionibacterium orla-jensen* 1909. In: *Bergey's Manual of Systematic Bacteriology*. Williams & Wilkins, Baltimore. Baltimore, pp. 1346–1353.
- de Melo Pereira, G.V., de Oliveira Coelho, B., Magalhães Júnior, A.I., Thomaz-Soccol, V., Soccol, C.R., 2018. How to select a probiotic? A review and update of methods and criteria. *Biotechnol. Adv.* 36, 2060–2076. <https://doi.org/10.1016/j.biotechadv.2018.09.003>.
- Dertli, E., Colquhoun, I.J., Gunning, A.P., Bongaerts, R.J., Le Gall, G., Bonev, B.B., Mayer, M.J., Narbad, A., 2013. Structure and biosynthesis of two exopolysaccharides produced by *Lactobacillus johnsonii* F19785. *J. Biol. Chem.* 288, 31938–31951. <https://doi.org/10.1074/jbc.M113.507418>.
- Deutsch, S.-M., Falentin, H., Dols-Lafargue, M., LaPointe, G., Roy, D., 2008. Capsular exopolysaccharide biosynthesis gene of *Propionibacterium freudenreichii* subsp. *shermanii*. *Int. J. Food Microbiol.* 125, 252–258.
- Deutsch, S.-M., Le Bivic, P., Hervé, C., Madec, M.-N., LaPointe, G., Jan, G., Le Loir, Y., Falentin, H., 2010. Correlation of the capsular phenotype in *Propionibacterium freudenreichii* with the level of expression of *gtf*, a unique polysaccharide synthase-encoding gene. *Appl. Environ. Microbiol.* 76, 2740–2746. <https://doi.org/10.1128/AEM.02591-09>.
- Deutsch, S.-M., Mariadassou, M., Nicolas, P., Parayre, S., Le Guellec, R., Chuat, V., Peton, V., Le Maréchal, C., Burati, J., Loux, V., Briard-Bion, V., Jardin, J., Plé, C., Folligné, B., Jan, G., Falentin, H., 2017. Identification of proteins involved in the anti-inflammatory properties of *Propionibacterium freudenreichii* by means of a multi-strain study. *Sci. Rep.* 7 (46409) <https://doi.org/10.1038/srep46409>.
- Deutsch, S.-M., Parayre, S., Bouchoux, A., Guyomarc'h, F., Dewulf, J., Dols-Lafargue, M., Baglinière, F., Cousin, F.J., Falentin, H., Jan, G., Folligné, B., 2012. Contribution of Surface β -Glucan polysaccharide to physicochemical and immunomodulatory properties of *Propionibacterium freudenreichii*. *Appl. Environ. Microbiol.* 78, 1765–1775. <https://doi.org/10.1128/AEM.07027-11>.
- Dobrurowska, J.M., Gerwig, G.J., Babuchowski, A., Kamerling, J.P., 2008. Structural studies on exopolysaccharides produced by three different propionibacteria strains. *Carbohydr. Res.* 343, 726–745. <https://doi.org/10.1016/j.carres.2007.12.006>.
- Fahs, A., Quilès, F., Jamal, D., Humbert, F., Francius, G., 2014. *In situ* analysis of bacterial extracellular polymeric substances from a *Pseudomonas fluorescens* biofilm by combined vibrational and single molecule force spectroscopies. *J. Phys. Chem. B* 118, 6702–6713. <https://doi.org/10.1021/jp5030872>.
- Falentin, H., Deutsch, S.-M., Jan, G., Loux, V., Thierry, A., Parayre, S., Maillard, M.-B., Dherbécourt, J., Cousin, F.J., Jardin, J., Sigulier, P., Couloux, A., Barbe, V., Vacherie, B., Wincker, P., Gibrat, J.-F., Gaillardin, C., Lortal, S., 2010. The complete genome of *Propionibacterium freudenreichii* CIRM-BIA1, a hardy actinobacterium with food and probiotic applications. *PLoS One* 5, e11748. <https://doi.org/10.1371/journal.pone.0011748>.
- Fang, H., Kang, J., Zhang, D., 2017. Microbial production of vitamin B12: a review and future perspectives. *Microb. Cell Factories* 16 (15). <https://doi.org/10.1186/s12934-017-0631-y>.
- Folligné, B., Deutsch, S.-M., Breton, J., Cousin, F.J., Dewulf, J., Samson, M., Pot, B., Jan, G., 2010. Promising immunomodulatory effects of selected strains of dairy propionibacteria as evidenced in vitro and in vivo. *Appl. Environ. Microbiol.* 76, 8259–8264. <https://doi.org/10.1128/AEM.01976-10>.
- Formosa Dague, C., Feuillie, C., Beaussart, A., Derclaye, S., Kucharíková, S., Lasa, I., Van Dijk, P., Dufrene, Y.F., 2016. Sticky matrix: adhesion mechanism of the staphylococcal polysaccharide intercellular adhesin. *ACS Nano* 10, 3443–3452. <https://doi.org/10.1021/acsnano.5b07515>.
- Francius, G., Alsteens, D., Dupres, V., Lebeur, S., De Keersmaecker, S., Vanderleyden, J., Gruber, H.J., Dufrene, Y.F., 2009. Stretching polysaccharides on live cells using single molecule force spectroscopy. *Nat. Protoc.* 4, 939–946. <https://doi.org/10.1038/nprot.2009.65>.
- Francius, G., Lebeur, S., Alsteens, D., Wildling, L., Gruber, H.J., Hols, P., Keersmaecker, S. D., Vanderleyden, J., Dufrene, Y.F., 2008. Detection, localization, and conformational analysis of single polysaccharide molecules on live bacteria. *ACS Nano* 2, 1921–1929. <https://doi.org/10.1021/nm800341b>.
- Fraunhofer, M.E., Jakob, F., Vogel, R.F., 2018. Influence of different sugars and initial pH on β -glucan formation by *Lactobacillus brevis* TMW 1.2112. *Curr. Microbiol.* 75, 794–802. <https://doi.org/10.1007/s00284-018-1450-z>.
- Galle, S., Arendt, E.K., 2014. Exopolysaccharides from sourdough lactic acid bacteria. *Crit. Rev. Food Sci. Nutr.* 54, 891–901. <https://doi.org/10.1080/10408398.2011.617474>.
- Ge, Y., Gong, M., Zadeh, M., Li, J., Abbott, J.R., Li, W., Morel, L., Sonon, R., Supekar, N. T., Azadi, P., Wang, Y., Jones, D.P., Li, S., Mohamadzadeh, M., 2020. Regulating colonic dendritic cells by commensal glycosylated large surface layer protein A to sustain gut homeostasis against pathogenic inflammation. *Mucosal Immunol.* 13, 34–46. <https://doi.org/10.1038/s41385-019-0210-0>.
- Horn, N., Wegmann, U., Dertli, E., Mulholland, F., Collins, S.R.A., Waldron, K.W., Bongaerts, R.J., Mayer, M.J., Narbad, A., 2013. Spontaneous mutation reveals influence of exopolysaccharide on *Lactobacillus johnsonii* surface characteristics. *PLoS One* 8, e59957. <https://doi.org/10.1371/journal.pone.0059957>.
- Joyce, E., Phull, S.S., Lorimer, J.P., Mason, T.J., 2003. The development and evaluation of ultrasound for the treatment of bacterial suspensions. A study of frequency, power and sonication time on cultured *Bacillus* species. *Ultrason. Sonochem.* 10, 315–318. [https://doi.org/10.1016/S1350-4177\(03\)00101-9](https://doi.org/10.1016/S1350-4177(03)00101-9).
- Kuyukina, M.S., Ivshina, I.B., Korshunova, I.O., Stukova, G.I., Krivoruchko, A.V., 2016. Diverse effects of a biosurfactant from *Rhodococcus ruber* IEGM 231 on the adhesion of resting and growing bacteria to polystyrene. *Amb. Express* 6 (14). <https://doi.org/10.1186/s13568-016-0186-z>.
- Landersjö, C., Yang, Z., Huttunen, E., Widmalm, G., 2002. Structural studies of the exopolysaccharide produced by *Lactobacillus rhamnosus* strain GG (ATCC 53103). *Biomacromolecules* 3, 880–884.
- Le Lay, C., Mounier, J., Vasseur, V., Weill, A., Le Blay, G., Barbier, G., Coton, E., 2016. In vitro and in situ screening of lactic acid bacteria and propionibacteria antifungal activities against bakery product spoilage molds. *Food Contr.* 60, 247–255. <https://doi.org/10.1016/j.foodcont.2015.07.034>.
- Lebeur, S., Vanderleyden, J., De Keersmaecker, S.C.J., 2008. Genes and molecules of lactobacilli supporting probiotic action. *Microbiol. Mol. Biol. Rev.* 72, 728–764. <https://doi.org/10.1128/MMBR.00017-08>. Table of Contents.
- Lebeur, S., Verhoeven, T.L.A., Francius, G., Schoofs, G., Lambrichts, I., Dufrene, Y., Vanderleyden, J., De Keersmaecker, S.C.J., 2009. Identification of a gene cluster for the biosynthesis of a long. Galactose-Rich Exopolysaccharide in *Lactobacillus rhamnosus* GG and Functional Analysis of the Priming Glycosyltransferase. *Appl. Environ. Microbiol.* 75, 3554–3563. <https://doi.org/10.1128/AEM.02919-08>.
- Lind, H., Jonsson, H., Schnürer, J., 2005. Antifungal effect of dairy propionibacteria—contribution of organic acids. *Int. J. Food Microbiol.* 98, 157–165. <https://doi.org/10.1016/j.ijfoodmicro.2004.05.020>.
- Malik, A.C., Reinbold, G.W., Vedamuthu, E.R., 1968. An evaluation of the taxonomy of *Propionibacterium*. *Can. J. Microbiol.* 14, 1185–1191.
- Marszałek, P.E., Dufrene, Y.F., 2012. Stretching single polysaccharides and proteins using atomic force microscopy. *Chem. Soc. Rev.* 41, 3523–3534. <https://doi.org/10.1039/c2cs15329g>.
- Martens, J.-H., Barg, H., Warren, M., Jahn, D., 2002. Microbial production of vitamin B12. *Appl. Microbiol. Biotechnol.* 58, 275–285. <https://doi.org/10.1007/s00253-001-0902-7>.
- McIntosh, M., Stone, B.A., Stanisch, V.A., 2005. Curdlan and other bacterial (1 \rightarrow 3)- β -D-glucans. *Appl. Microbiol. Biotechnol.* 68, 163–173. <https://doi.org/10.1007/s00253-005-1959-5>.
- Mende, S., Rohm, H., Jaros, D., 2016. Influence of exopolysaccharides on the structure, texture, stability and sensory properties of yoghurt and related products. *Int. Dairy J.* 52, 57–71. <https://doi.org/10.1016/j.idairyj.2015.08.002>.
- Nordmark, E.-L., Yang, Z., Huttunen, E., Widmalm, G., 2005. Structural studies of the exopolysaccharide produced by *Propionibacterium freudenreichii* ssp. *shermanii* JS. *Biomacromolecules* 6, 521–523.

- O'Toole, G.A., 2011. Microtiter dish biofilm formation assay. *JoVE*. <https://doi.org/10.3791/2437>.
- Pham, D.K., Ivanova, E.P., Wright, J.P., Nicolau, D.V., 2003. AFM analysis of the extracellular polymeric substances (EPS) released during bacterial attachment on polymeric surfaces. In: Nicolau, D.V., Enderlein, J., Leif, R.C., Farkas, D.L. (Eds.), Presented at the Biomedical Optics 2003, p. 151. <https://doi.org/10.1117/12.485876>. San Jose, CA.
- Pogacic, T., Maillard, M.-B., Leclerc, A., Herve, C., Chuat, V., Yee, A.L., Valence, F., Thierry, A., 2015. A methodological approach to screen diverse cheese-related bacteria for their ability to produce aroma compounds. *Food Microbiol.* 46, 145–153. <https://doi.org/10.1016/j.fm.2014.07.018>.
- Polak-Berecka, M., Choma, A., Waško, A., Górska, S., Gamian, A., Cybulska, J., 2015. Physicochemical characterization of exopolysaccharides produced by *Lactobacillus rhamnosus* on various carbon sources. *Carbohydr. Polym.* 117, 501–509. <https://doi.org/10.1016/j.carbpol.2014.10.006>.
- Rabah, H., Rosa d Carmo, F.L., Jan, G., 2017. Dairy Propionibacteria: Versatile Probiotics. *Microorganisms* 5 (24). <https://doi.org/10.3390/microorganisms5020024>.
- Rajagopal, M., Walker, S., 2017. Envelope structures of gram-positive bacteria. *Curr. Top. Microbiol. Immunol.* 404, 1–44. https://doi.org/10.1007/82_2015_5021.
- Scholz, C.F.P., Kilian, M., 2016. The natural history of cutaneous propionibacteria, and reclassification of selected species within the genus *Propionibacterium* to the proposed novel genera *Acidipropionibacterium* gen. nov., *Cutibacterium* gen. nov. and *Pseudopropionibacterium* gen. nov. *Int. J. Syst. Evol. Microbiol.* 66, 4422–4432. <https://doi.org/10.1099/ijsem.0.001367>.
- Tareb, R., Bernardeau, M., Amiel, C., Vernoux, J.P., 2017. Usefulness of FTIR spectroscopy to distinguish rough and smooth variants of *Lactobacillus farciminis* CNCM-I-3699. *FEMS Microbiol Lett* 364. <https://doi.org/10.1093/femsle/fnw298>.
- Tareb, R., Bernardeau, M., Horvath, P., Vernoux, J.-P., 2015. Rough and smooth morphotypes isolated from *Lactobacillus farciminis* CNCM I-3699 are two closely-related variants. *Int. J. Food Microbiol.* 193, 82–90. <https://doi.org/10.1016/j.ijfoodmicro.2014.08.036>.
- Thierry, A., Deutsch, S.-M., Falentin, H., Dalmaso, M., Cousin, F.J., Jan, G., 2011. New insights into physiology and metabolism of *Propionibacterium freudenreichii*. *Int. J. Food Microbiol.* 149, 19–27. <https://doi.org/10.1016/j.ijfoodmicro.2011.04.026>.
- Thierry, A., Maillard, M.B., Herve, C., Richoux, R., Lortal, S., 2004. Varied volatile compounds are produced by *Propionibacterium freudenreichii* in Emmental cheese. *Food Chem.* 87, 439–446. <https://doi.org/10.1016/j.foodchem.2003.12.018>.
- Tinzl-Malang, S.K., Rast, P., Grattepanche, F., Sych, J., Lacroix, C., 2015. Exopolysaccharides from co-cultures of *Weissella confusa* 11GU-1 and *Propionibacterium freudenreichii* JS15 act synergistically on wheat dough and bread texture. *Int. J. Food Microbiol.* 214, 91–101. <https://doi.org/10.1016/j.ijfoodmicro.2015.07.025>.
- Tripathi, P., Dupres, V., Beaussart, A., Lebeer, S., Claes, I.J.J., Vanderleyden, J., Dufrene, Y.F., 2012. Deciphering the nanometer-scale organization and assembly of *Lactobacillus rhamnosus* GG pili using atomic force microscopy. *Langmuir* 28, 2211–2216. <https://doi.org/10.1021/la203834d>.
- von Freudenreich, E., Orla-Jensen, O., 1906. Über die in Emmentalerkäse stattfindende Propionsäure-gärung. *Zentralbl. Bakteriol.* 17, 529–546.
- Walling, E., Gindreau, E., Lonvaud-Funel, A., 2005. A putative glucan synthase gene dps detected in exopolysaccharide-producing *Pediococcus damnosus* and *Oenococcus oeni* strains isolated from wine and cider. *Int. J. Food Microbiol.* 98, 53–62. <https://doi.org/10.1016/j.ijfoodmicro.2004.05.016>.
- Wang, C., Ehrhardt, C.J., Yadavalli, V.K., 2015. Single cell profiling of surface carbohydrates on *Bacillus cereus*. *J. R. Soc. Interface* 12. <https://doi.org/10.1098/rsif.2014.1109>, 20141109.
- Yee, A.L., Maillard, M.-B., Roland, N., Chuat, V., Leclerc, A., Pogacic, T., Valence, F., Thierry, A., 2014. Great interspecies and intraspecies diversity of dairy propionibacteria in the production of cheese aroma compounds. *Int. J. Food Microbiol.* 191, 60–68. <https://doi.org/10.1016/j.ijfoodmicro.2014.09.001>.
- Zhao, W., Yang, S., Huang, Q., Cai, P., 2015. Bacterial cell surface properties: role of loosely bound extracellular polymeric substances (LB-EPS). *Colloids Surf. B Biointerfaces* 128, 600–607. <https://doi.org/10.1016/j.colsurfb.2015.03.017>.